



Contents lists available at [SciVerse ScienceDirect](#)

Catalysis Today

journal homepage: www.elsevier.com/locate/cattod



Controlled Pd deposition on fibers by electroless plating. The effects of the support on the reduction of nitrite in water

M.L. Bosko, F.A. Marchesini, L.M. Cornaglia, E.E. Miró*

Instituto de Investigaciones en Catálisis y Petroquímica (FIQ, UNL-CONICET), Santiago del Estero 2829, 3000 Santa Fe, Argentina

ARTICLE INFO

Article history:

Received 22 March 2012
Received in revised form 1 November 2012
Accepted 25 December 2012
Available online xxx

Keywords:

Pd supported on fibers
Nitrite reduction
Water purification
Electroless plating
Selectivity to N₂

ABSTRACT

Pd catalysts supported on activated silica–alumina fibers (CFs) and activated carbon felts (ACFs) were prepared and evaluated for the reduction of nitrite in water in a batch reactor. The electroless plating (ELP) method was used in order to deposit small Pd particles on the surface of the fibers. While a homogeneous distribution of Pd nanoparticles was obtained for carbon fibers, this was not the case for ceramic ones in which non-homogeneous patches of Pd films were formed. This fact resulted in a higher activity for nitrite reduction when carbon fibers were used. However, the selectivity toward the undesired product ammonia, measured at the end of the reaction, was slightly higher for Pd/ACFs catalysts.

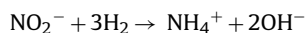
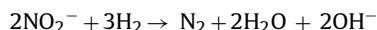
© 2013 Elsevier B.V. All rights reserved.

1. Introduction

Due to shifting demands and new environmental requirements, the development of novel materials with applications in the area of catalysis has become a great research challenge. The selection of both the preparation method and the support is especially important since these are key parameters to explore in the design of these solids. To procure a high availability of the active sites on the catalyst surface, it is fundamental to deposit small metallic particles (nm-sized) with high uniformity, electroless plating (ELP) being a valuable technique for this purpose [1]. ELP is an auto-catalytic process by which a chemical reducing agent reduces a metallic salt onto specific surface sites of the catalytic surface [2]. On the other hand, cloths and felts as well as monoliths and other structured supports have advantages with respect to conventional ones. They allow overcoming the inherent diffusional limitations and improving the accessibility of the internal regions of the material to reactants and products. Besides, they reduce the pressure drop in reactors.

In a previous work [1], we prepared Pd catalysts on activated carbon felts (ACFs) by electroless plating. These catalysts were applied to the nitrite reduction reaction in water. Nitrite and nitrate are water pollutants, and catalysts containing noble metals have been extensively studied for their abatement through reduction

processes. The reaction scheme for nitrite reduction by hydrogen is shown below:



It can be observed that nitrogen and ammonia are the reaction products [3]. At present, the mechanism of N₂ formation is unclear, but the most frequently suggested mechanism involves dimerization of NO_(dis) with N₂O as an intermediate [4].

The synthesized solids were active to nitrite reduction and exhibited high selectivity to N₂ which increased with reaction time. When the Pd load was ca. 1.8 wt.%, the morphology showed a good uniformity of particles with small size (130–210 nm) [1]. It is well known that nitrogen formation strongly depends on both the chemical properties of the catalyst used and mass-transport phenomena [5]. In this vein, Marchesini et al. [6] reported the highest activity in catalysts that have their Pd active sites on Al₂O₃ and they observed that the use of SiO₂ as support improves the selectivity to gaseous nitrogen compounds. Thus, mixtures of Al₂O₃ + SiO₂ resulted in enhanced values of both activity and selectivity.

The aim of this study is to compare the support effect on the catalytic performance for the nitrite reduction in water using different types of fibers as structured supports. For this purpose, we selected activated carbon felts and ceramic fibers as supports and ELP was chosen as preparation method. The ELP conditions were varied in order to investigate their influence on the Pd morphology

* Corresponding author. Tel.: +54 342 453 6861; fax: +54 342 4536861.
E-mail addresses: emiro@fiq.unl.edu.ar, cabemiro@hotmail.com (E.E. Miró).

and catalytic properties. Scanning electron microscopy (SEM), X-ray photoelectron spectroscopy (XPS), and X-ray diffraction (XRD) were the characterization techniques selected and the catalytic measurements were carried out in a stirred batch reactor.

2. Experimental

2.1. Supports

Two kinds of fibers were used as supports: ceramic fibers (63–64 wt.% SiO₂, 35–36 wt.% Al₂O₃ and 0.327 wt.% Fe and 0.221 wt.% Ti as impurities) obtained by elutriation of ceramic cloth purchased from Carbo San Luis S.A. and activated carbon felts provided by American Technical Trading, Inc. with a content of impurities equal to 1.5 wt.% (Mg: 0.06; Ca: 0.30; K: 0.435; Si: 0.165; P: 0.075; Cr: 0.024; Al: 0.0375; S: 0.0508; Ti: 0.018; Cl: 0.165; Fe + Sn + Zn balance) [7].

2.2. Preparation of catalytic fibers

The ceramic fibers (CFs) were calcined in stagnant air for 4 h at 500 °C; and the activated carbon felts (ACFs) were pre-treated in an aqueous solution of HCl 4.8 M at 50 °C for 2 h and then rinsed in distilled water and dried at 80 °C overnight. After that, the Pd/fibers were prepared in two steps. First, the surfaces were activated by deposition of catalytic Pd seed nuclei [1]. The fibers were activated by the conventional two-step SnCl₂/PdCl₂ method [8]. Substrates were immersed 5 min in solutions of SnCl₂·2H₂O (pH 2) and then of PdCl₂ (pH 2); this sequence was considered as an activation cycle. After the activation, the metallic electroless plating (ELP) procedure was carried out in order to grow the Pd nuclei. The fibers were immersed in the plating bath for 90 min at 50 °C. The as-deposited ones were carefully rinsed with deionized water and finally dried at 80 °C.

Three samples on ACFs (A1, B1 and C1) and four on CFs (A2, B2, C2 and D2) were prepared by this technique. The synthesis features and Pd loadings are shown in Table 1.

2.3. Catalysis characterization

2.3.1. X-ray diffraction (XRD)

The XRD patterns of the films were obtained with an XD-D1 Shimadzu instrument, using Cu K α radiation at 30 kV and 40 mA. The scan rate was 2° min⁻¹ in the range 2 θ = 10–90°.

Table 1
Synthesis features and Pd loading of the prepared samples.

Samples	Activated carbon felts			Ceramic fibers			
	A1	B1	C1	A2	B2	C2	D2
<i>Composition of activation solutions</i>							
SnCl ₂ ·2H ₂ O (g/L)	0.13	0.13	0.13	0.13	0.35	0.35	0.35
PdCl ₂ (g/L)	0.10	0.10	0.10	0.10	0.25	0.25	0.25
Number of activation cycles	1	4	4	4	6	6	7
<i>Composition of plating baths</i>							
PdCl ₂ (g/L)	0.09	0.45	0.9	0.45	1.4	1.8	2
Na ₂ EDTA (g/L)	10.0	8.5	16.8	8.5	26.0	34.0	36.0
NH ₄ OH (28%) (mL/L)	100	80	160	80	260	320	360
N ₂ H ₄ (0.25 M) (mL/L)	0.90	5	10	–	–	–	–
N ₂ H ₄ (0.41 M) (mL/L)	–	–	–	3	9.3	12	13.3
pH	11	11	11	11	11	11	11
Theoretical Pd (wt.%) ^a	3.0	15.0	30.0	5.1	15.8	20.3	22.5
Pd (wt.%) ^b	0.14	1.80	1.90	0.52	3.90	15.30	17.50
Deposition yield % ^c	4.7	12.0	6.3	10.2	24.7	75.4	77.8

^a Defined as Pd mass in the plating bath · 100/mass of support.

^b Data obtained by ICP analysis.

^c Defined as [Pd load (obtained by ICP)/Pd theoretical load] × 100.

2.3.2. Scanning electron microscopy (SEM)

The images were obtained using a JEOL scanning electron microscope; model JSM-35 C, equipped with an energy dispersive analytical system (EDS, EDAXTM).

2.3.3. X-ray photoelectron spectroscopy (XPS)

X-ray photoelectron spectroscopy (XPS) analyses were performed in a multi-technique system (SPECS) equipped with a dual Mg/Al X-ray source and a hemispherical PHOIBOS 150 analyzer operating in the fixed analyzer transmission (FAT) mode. The spectra were obtained with a pass energy of 30 eV and the Mg-K α X-ray source was operated at 100 or 200 W. The working pressure in the analyzing chamber was less than 2 × 10⁻⁹ kPa. The XPS analyses were performed on the fresh and used catalysts pre-treated in the load-lock chamber in a flowing H₂/Ar mixture for 1 h. The spectral Pd 3d, Sn 3d, Al 2p, Si 2p and C 1s were recorded. The data treatment was performed with the Casa XPS program (Casa Software Ltd., UK). The peak areas were determined by integration employing a Shirley-type background. For the quantification of the elements, sensitivity factors provided by the manufacturer were used.

2.3.4. Inductively coupled plasma (ICP)

Volumetric chemical analyses were performed using the inductively coupled plasma technique with a Perkin Elmer P-40 instrument.

2.4. Activity test

The catalytic reduction of nitrite was performed in a three-necked round bottom flask (volume 250 mL) equipped with a magnetic stirrer (700–800 rpm). The pH value was controlled with an automatic pH controller unit. Experiments were carried out at room temperature, pH 5 and atmospheric pressure. Hydrogen was fed into the solution through a tube. The stirred batch reactor was loaded with 80 or 120 mL of distilled water, 200 or 300 mg of catalyst, and normally 100 N-ppm of nitrite as initial concentration. Subsequently, a hydrogen flow of 400 mL min⁻¹ was fed to the batch reactor. The pH was maintained during the reaction time by the addition of small amounts of a HCl (~0.01 M) solution [9]. Before the reaction test, only the Pd/ACFs were reduced in a stream of H₂ at 100 °C. This pretreatment was standard in previous studies. However, we observed that the same results were obtained with or without the reduction pretreatment. Thus, for the sake of simplicity, we decided not to perform this pretreatment for the ceramic fibers.

Small samples were taken from the vessel for the determination of nitrite and ammonium using Vis spectroscopy (Cole Parmer 1100 Spectrophotometer) combined with colorimetric reagents. The colorimetric Gries reaction was used in the assay for nitrites. Ammonium was analyzed by the adapted Berthelot method. Nitrite conversions were calculated as the amount of nitrite consumed at different reaction times divided by the initial nitrite concentration. The selectivity to N_2 was defined as the amount of N_2 produced (considering NH_4^+ and N_2 as the main products) divided by the initial concentration of nitrites [10]. Other species such as NO and N_2O are negligible due to the rapid reduction into N_2 when palladium catalysts are used [4]. For some selected samples, three consecutive nitrite pulses were fed in order to evaluate the catalysts stability.

Results are expressed as NO_2^- conversion (X , %), selectivity ammonium ($S_{NH_4^+}$, %) and selectivity to nitrogen (S , %). These parameters are defined as follows:

$$X (\%) = \left[1 - \frac{C}{C_0} \right] \times 100$$

$$S_{NH_4^+} (\%) = \left[\frac{C_{NH_4^+}}{C_0 - C} \right] \times 100$$

where C_0 is the initial concentration of nitrites (mg/L, $N-NO_2^-$), C is the nitrites concentration at time t , and $C_{NH_4^+}$ is the ammonium concentration at time t . Selectivity to gaseous nitrogenated compounds ($N_{2(g)}$) and a small amount of N_2O) is defined as:

$$S_{N_2} (\%) = 100 - S_{NH_4^+} (\%)$$

3. Results and discussion

3.1. Catalysts characterization

Different samples were prepared by electroless plating (see Table 1), the number of activation cycles and the Pd content in the activation and plating solutions were modified in order to study their effects on the catalytic performance. The edta and ammonium varied with Pd content to ensure the complex formation, except for catalyst A1 in which higher concentrations of these components were necessary to obtain a stable complex at the bath temperature. The (metal/hydrazine) stoichiometric ratio equal to 2:1 was maintained in all baths [11].

Additionally, for the ceramic supports, we needed to increase the Pd concentration, in order to improve the catalytic performance. And we decided also to increase the activation cycles to obtain most Pd nuclei, besides higher Pd content. The reasons for the different conditions selected are related to the different characteristics of the fibers. Note that the volume/mass ratio of the carbon support is higher than that of the ceramic one; hence, the bath concentrations require to be modified to obtain a given Pd mass/support mass ratio. It can be seen that A2 and B2 have identical activation and plating bath composition, but the Pd mass in the plating bath. 100/mass of support were 15% and 5.1% for carbon and ceramic supports, respectively.

The XPS data are shown in Table 2. The binding energy for the Pd $3d_{5/2}$ feature did not present a significant shift with respect to that of metallic Pd ($BE = 335.1 \pm 0.1$ eV) [12], and only the catalysts C2 and D2 showed energies slightly less than 335 eV. This value corresponds to pure Pd [13], suggesting that Pd was not oxidized when the solids were exposed to ambient conditions.

Taking into account that the major elements of ceramic fibers are Al, Si and O, it is clear that the surface mass Pd/(Al+Si) ratio is higher than the Pd/support ratio. Now, comparing those values with the bulk contents (Table 1), it can be claimed that the bulk Pd contents are higher than the superficial ones (Table 2). Instead for

Table 2
Surface (XPS) and features of Pd/ACFs and Pd/CFs.^{a,b}

Catalysts	Pd $3d_{5/2}$ (eV)	Pd/C	Pd/(Al + Si)	Pd/Sn
Sample A1	335.5	0.13	–	3.02
Used	335.5	0.07	–	1.59
Sample B1	335.3	1.86	–	31.17
Used	335.4	0.69	–	6.67
Sample C1	335.4	1.79	–	58.78
Used	335.3	1.57	–	34.15
Sample A2	335.3	–	0.07	0.34
Used	335.5	–	0.02	0.29
Sample B2	335.4	–	0.91	1.23
Used	335.2	–	0.37	1.21
Sample C2	335.0	–	3.43	21.92
Used	334.7	–	0.55	8.71
Sample D2	335.2	–	5.88	10.50
Used	334.8	–	0.73	4.68

^a The catalysts were treated in the spectrometer reaction chamber at room temperature with a 5% H_2/Ar flow.

^b Ratio of mass concentrations.

the carbon support, the solids showed a similar Pd content in both levels.

This suggests that Pd has greater affinity for the carbon surface compared to the ceramic one. On the other hand, with the exception of solid C2, the surface mass Pd/Sn ratio increases with the Pd content in the plating baths. These noticeable amounts of Sn are incorporated to the fibers due to its presence in the solution employed for the activation cycles. Nevertheless, the presence of Sn does not negatively affect the catalytic behavior. Moreover, it could be beneficial when nitrate is used as reactive instead of nitrite [14].

After the reaction test, no loss of Pd was detected and the bulk metal concentration remained constant in all samples, as measured by inductively coupled plasma-atomic emission spectrometry (not shown). However, the XPS results indicate that the Pd surface concentration decreases in all samples (Table 2), probably due to the sinterization of Pd crystals or metal migration inside the support pores [1].

On the other hand, Table 1 shows the deposition yields or plating efficiencies, defined as the % ratio of the Pd load (obtained by ICP) and Pd theoretical load. Note that the plating efficiency increased with the palladium content. This behavior is expected when there are neither diffusional limitations nor limiting reagents [11,15].

The SEM images (Figs. 1 and 2) show the morphologies of the different samples. The images at low magnification show a μm -size between 10 and 15 for the AC fibers (Fig. 1a–c); instead, the CFs showed a large size distribution of the fibers, with an average size of 2.8 μm (Fig. 2a–d).

The SEM images of catalysts (on ACFs) show homogenous deposition of Pd particles for solids A1 and B1 (Fig. 1d–e and g–h) and the incipient formation of a thin layer on sample C1 (Fig. 1f and i). When the Pd load was equal to 0.14 wt.%, a homogeneous dispersion of Pd particles with a crystal size distribution between 65 and 150 nm was observed (Fig. 1d and g). Sample B1 also showed a homogenous dispersion and a good quantity of the Pd particles, but with larger particle size between 130 and 210 nm (Fig. 1e and h). The average size estimated for samples A1 and B1 was equal to 96 and 169 (Fig. 1) with 95% confidence intervals of 86–106 nm and 160–179 nm, respectively, as shown in the inserts of Fig. 1g and h [1]. However, on the ceramic support, only sample A2, with a Pd load of 0.52 wt.% shows some particles with an incipient formation of a thin layer (Fig. 2). In the other samples, Pd was deposited as films, but only on some fibers, resulting in an inhomogeneous deposition (Fig. 2). Probably, certain nuclei on the ceramic support that were formed could be unstable because there are no metallic bonds between the ceramic support and the Pd seeds [16].

After reaction, the particles of solid A1 and B1 showed two effects that can be observed in the SEM images: the size of the

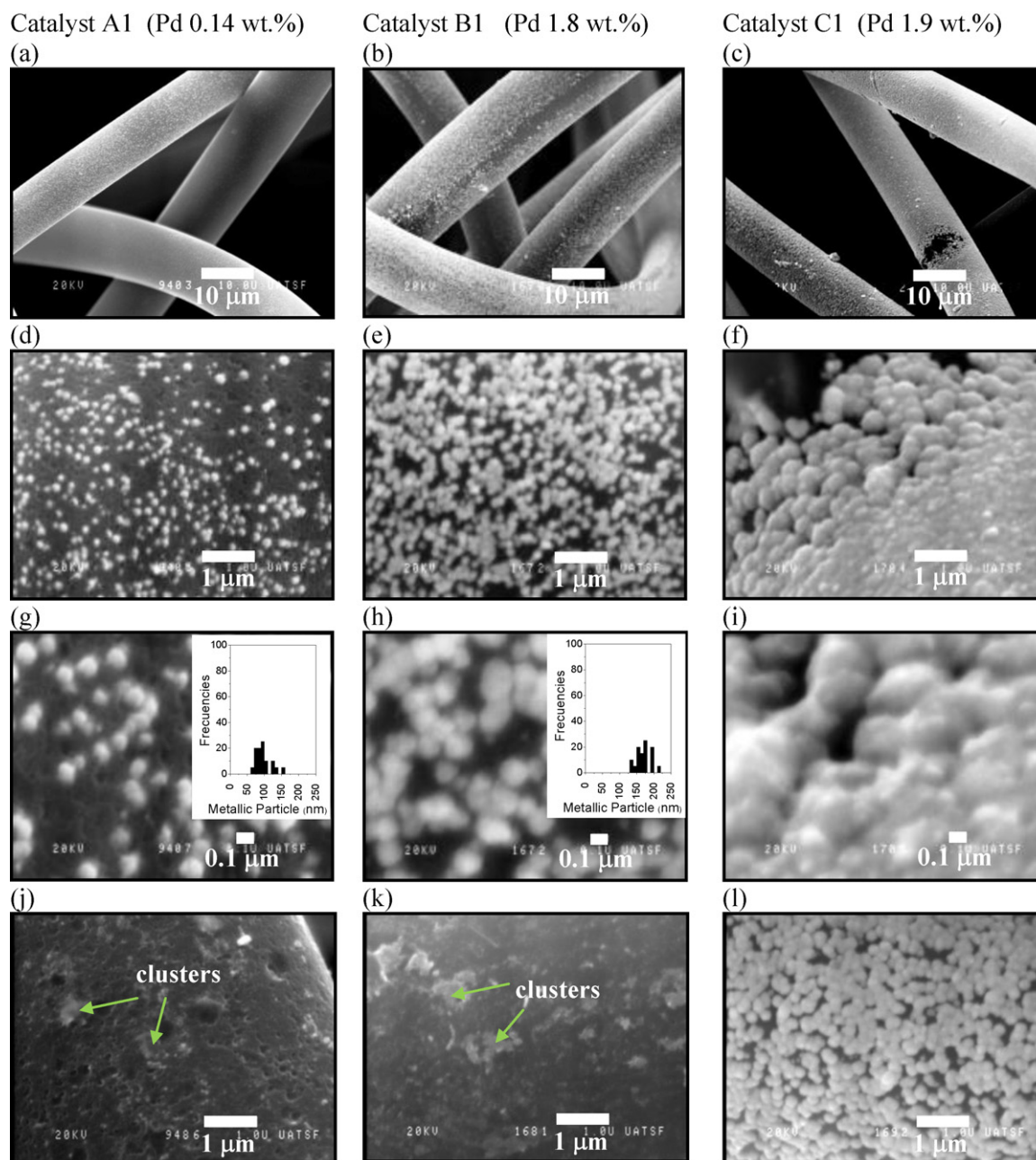


Fig. 1. Magnified view of fibers with different Pd loading for fresh (a–i) and used (j–l) catalysts on activated carbon support.

Pd particles grew, and a probable migration of Pd inside the AC pores (Fig. 1j and k) [1] in agreement with the XPS results (Table 2). Instead, for the ceramic support, in samples B2, C2 and D2, the films were still observed on the surfaces (Fig. 2n–p) but for sample A2 it can be observed that the Pd particles grew (Fig. 2m).

The XRD patterns of fresh Pd/ACF and Pd/FC catalysts are shown in Fig. 3. Samples B (1 and 2), C (1 and 2) and D2 showed all expected reflections of palladium face-centered cubic (fcc) structure [Pd: PDF 46-1043]. These reflections appear at 39.9°, 46.4°, 67.8°, 81.9° and 86.6°, for the (1 1 1); (2 0 0); (2 2 0); (3 1 1); and (2 2 2), respectively. Pd reflection peaks do not appear in catalyst A1, which has a Pd load of 0.14 wt.%. However, for a load of 0.52 wt.% (A2), the Pd (1 1 1) plane can be displayed. The different peak intensities are in agreement with the different Pd load of the samples (Table 1). Note that for all samples, palladium oxide signals are not observed, which

suggests that this metal is in the reduced form despite the exposure to air.

3.2. Reaction studies

The nitrite reduction results under hydrogen atmosphere at room temperature (pH 5) are presented in the next paragraphs. It should be pointed out that, since the rate of nitrite conversion and that of ammonia formation are strongly dependent on the acidity of the aqueous media, the pH must be carefully controlled [17]. We selected a pH of 5 because in a previous work we found that it represents an optimum value [1,18].

The Pd/ACFs were reduced before the reaction runs in a stream of H₂ at 100 °C. This step was omitted for the Pd/CFs because, in previous experiments performed with the solid D2, similar activities and selectivities were obtained for both the reduced and unreduced

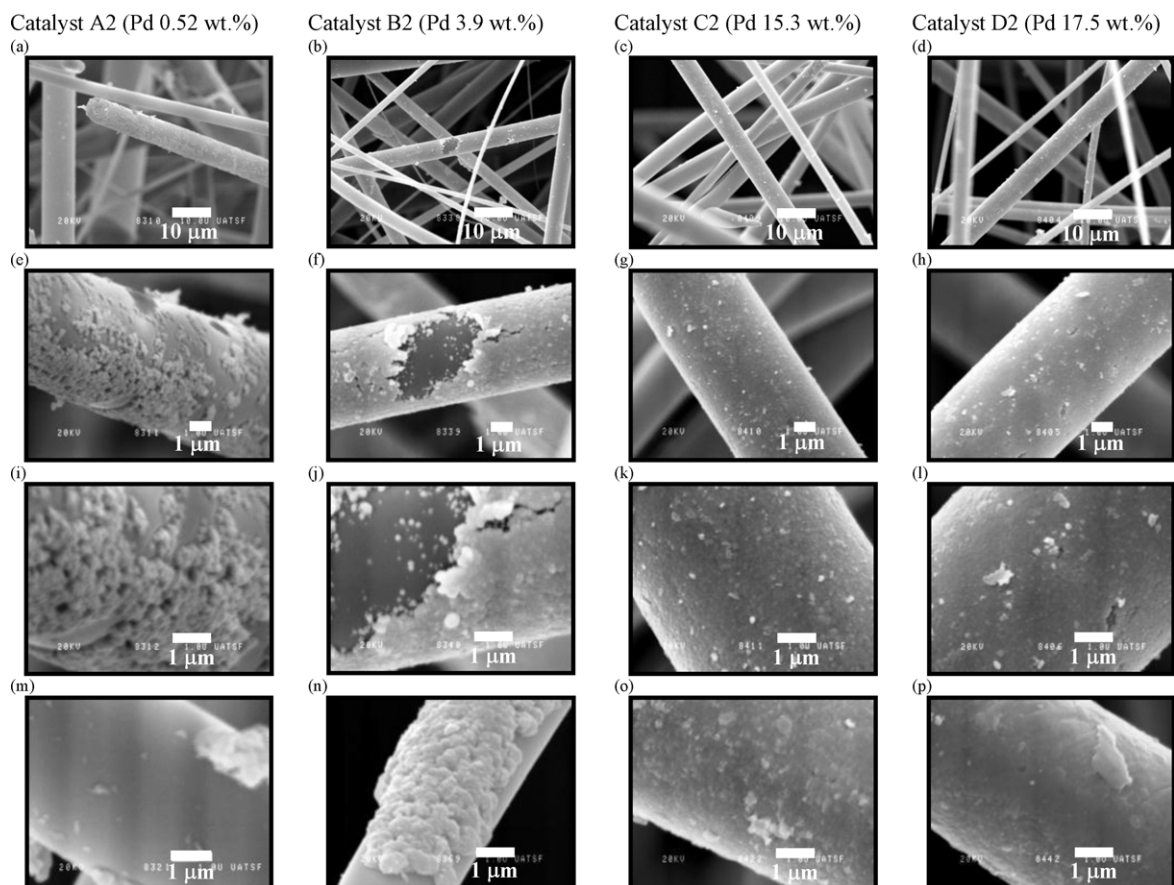


Fig. 2. Magnified view of fibers with different Pd loading for fresh (a–l) and used (m–p) catalysts on ceramic support.

catalysts (Table 3 and Fig. 6). Taking into account that the palladium by electroless plating is deposited in its reduced form, this behavior was predictable [1]. Moreover, it has been reported by other authors that the pretreatment in hydrogen at 100 °C does not provoke sintering and/or formation of alloys [19–22].

In Table 3, it can be observed that the most active catalysts were B1 and C1. The nitrites are totally consumed in just 40 min for sample B1, whereas sample C1 required a time of slightly more

than 75 min for the complete consumption of 100 N–ppm of nitrite. These results are in agreement with the SEM images (Fig. 1) where it can be observed that sample B1 presents homogeneous deposition of great quantity of Pd particles with small size. Instead, when Pd was deposited on the ceramic support, the activities were lower. The nitrites were consumed in 120 min for sample C2, and only remained 4.1 N–ppm NO_2^- for sample D2 (Table 3) when the solids were not reduced. The lower activity of this substrate for the nitrite

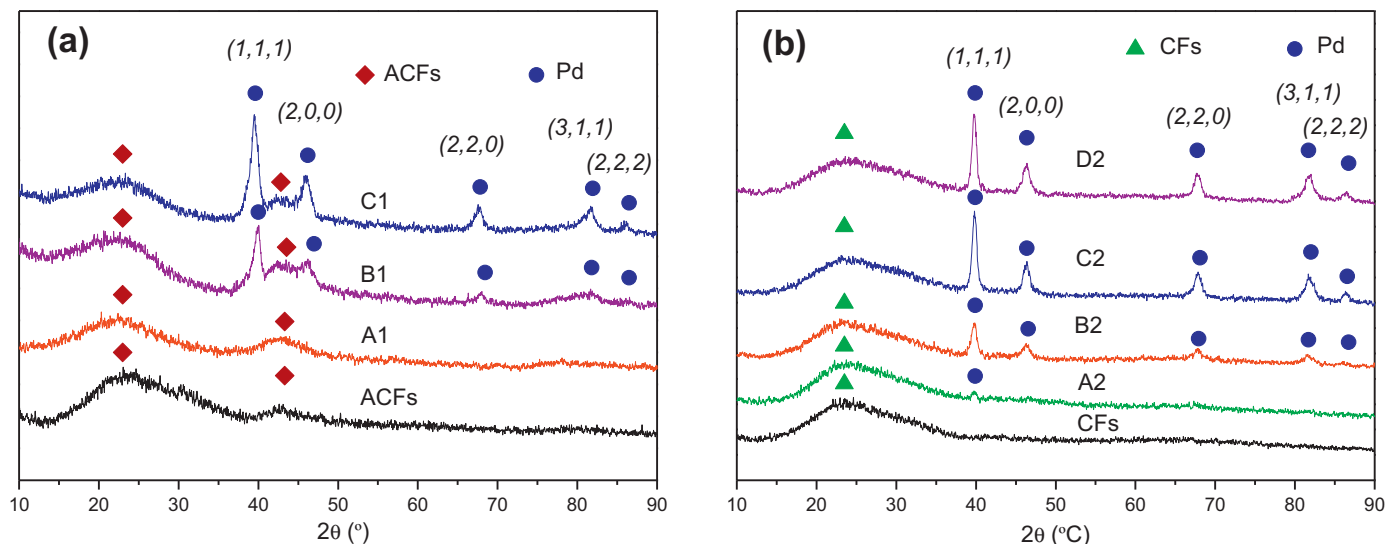


Fig. 3. XRD patterns of fresh Pd catalysts on ACFs (a) and CFs (b).

Table 3
Summary of reaction results.

Sample	Pulse ^c	Initial N-ppm NO ₂ ⁻	Time (min)	NO ₂ ⁻ conversion (%)	Residual N-ppm NH ₄ ⁺
ACFs ^a	I	100	120	17.7	nd ^d
A1 ^a	I	100	120	55.6	nd ^d
B1 ^a	I	25	30	100	6.1
B1 ^a	II	50	30	100	18.3
B1 ^a	III	100	40	100	5.1
C1 ^a	I	100	75	100	42.2
C1 ^a	II	100	75	95.5	8.2
C1 ^a	III	100	75	92.7	7.9
CFs ^b	I	100	120	16.3	nd ^d
A2 ^b	I	100	120	14.0	nd ^d
B2 ^b	I	100	120	73.0	nd ^d
C2 ^b	I	100	120	100.0	1.2
C2 ^b	II	100	120	100.0	2.3
C2 ^b	III	100	120	100.0	2.1
D2 ^b	I	100	120	95.9	5.8
D2 ^a	I	100	120	99.4	3.5

^a Before the reaction, the catalyst were reduced 1 h in H₂ atmosphere at 100 °C.

^b These catalysts were not reduced.

^c I, II, III indicate consecutive nitrite pulses fed into the batch reactor.

^d Not detected.

reduction reaction could be due to the low availability of Pd surface sites on the films (Fig. 2). In relation to the other samples (A1, A2 and B2), they required more time for total conversion of nitrites (Table 3). In Table 3, it can be observed that the supports display some slight NO₂⁻ reduction activity, which can be ascribed to the existence of some active species provided by metallic impurities.

The supports showed different behaviors accounting for the selectivity to N₂. For the case of activated carbon, after a certain reaction time the ammonium production ceased. Probably the ammonium itself inhibits the active sites responsible for its formation. For example, solid B1 exhibited residual concentrations of ammonia of 18.3 ppm and 5.1 ppm (Table 3) for the second and third pulses, respectively. Instead, the ceramic fiber always showed high selectivity to N₂ from the beginning of the reaction. The residual N-ppm NH₄⁺ for sample D2 (without previous reduction) was equal to 5.8. This value was higher than 1.2 N-ppm NH₄⁺, which was obtained for solid C2. This behavior could suggest that the major Pd load (17.5 wt.%) in solid D2 favors the reaction displacement at ammonium production. Note that the residual N-ppm NH₄⁺ for catalyst C2, is very close to the limit value of 0.5 ppm of the European Union legislation [23].

The major selectivity to ammonia in the carbon based catalyst supports is in agreement with results reported by Chinthaginjala et al. [3]. They found that these catalysts were more selective toward ammonia as compared to oxidic supports.

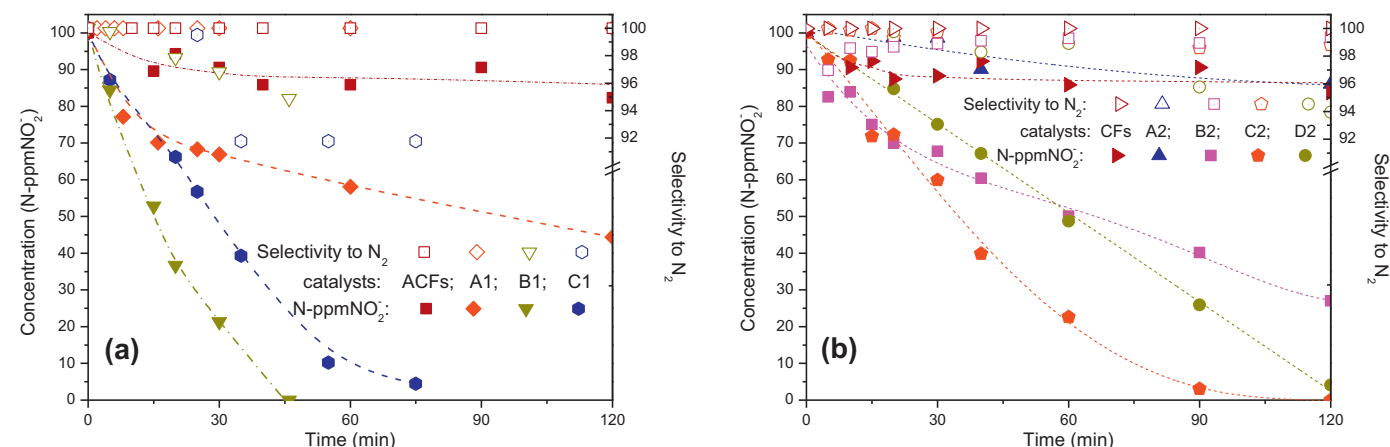


Fig. 4. Effect of the Pd loading on nitrite conversion and the selectivity to N₂ on ACFs (a) and CFs (b).

Fig. 4 shows the nitrite conversions and selectivities to N₂ at different times for activated carbon (a) and ceramic fibers (b). From Fig. 4a, we estimated the reaction rates for samples A1 and B1 at 30 min; the values were 1.4×10^{-3} and 8.8×10^{-4} mmol NO₂⁻/L min cm². These values were calculated by dividing the slope of the curves in Fig. 4 by the exposed Pd surface calculated from SEM data. The calculated exposed surfaces were 5.4 and 3.0 m² g⁻¹ Pd for samples A1 and B1, respectively, with 95% confidence intervals of 4.9–5.9 m² g⁻¹ Pd and 2.8–3.2 m² g⁻¹ Pd. Considering the difference in particle size of these two solids (96 and 169 nm), it could be considered that this parameter does not affect the specific reaction rate strongly [1]. When the ceramic fibers were used as supports, it can be noted that C2 is the more active sample. As a matter of fact, while the NO₂⁻ conversion was 97%, for C2, a value of 74%, was obtained for sample D2. In both cases conversions were measured at 90 min of time-on-stream.

If we compare the results obtained in this work with those reported by Soares et al. [24] for a standard Pd/activated carbon catalyst under similar reaction conditions, they report a somewhat higher nitrate conversion (85%) at 120 min of reaction as compared with our catalyst A1 (56%). However, while at that time ammonia was not detected in our catalyst, a selectivity of 82% was reported in theirs. Thus, our catalyst is somewhat less active, but much more selective.

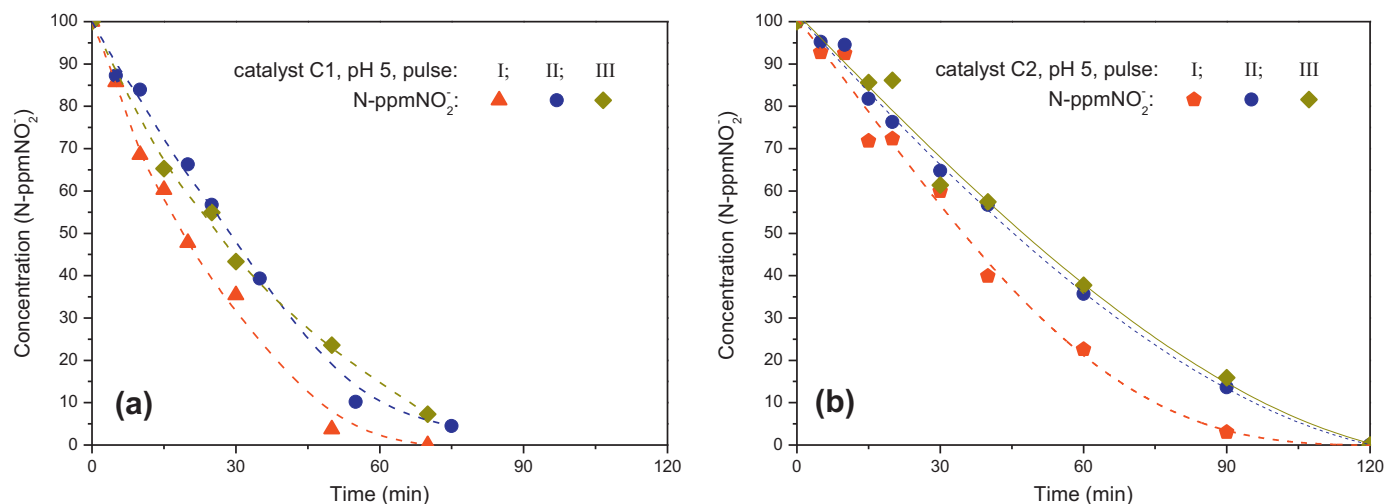


Fig. 5. Stability of the C1 (a) and C2 (b) catalysts.

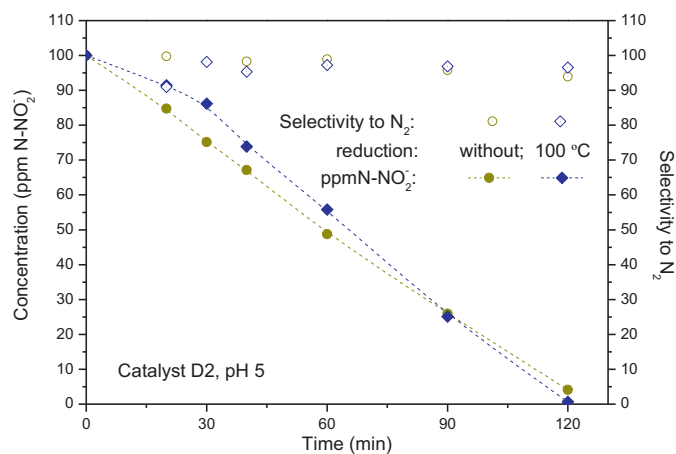


Fig. 6. Catalytic performance of the D2 with and without reduction.

To study the effect of time-on-stream over the catalyst activity, a previously designed experiment [25] was performed. In this one, when the nitrite amount (pulse) is totally converted a new pulse is introduced in the batch reactor.

Fig. 5 displays the performance of catalysts C1 and C2, when three consecutive pulses of nitrite (N-100 ppm) were introduced in the reaction media. Note that for both solids, the time required to reach a NO₂⁻ conversion of 100%, in the second and third pulse of nitrite, only slightly increased as compared with the first one. These results suggest that these solids display a slow deactivation with time under practical conditions, which can be originated by the sinterization of Pd crystals when exposed to the aqueous reaction media [1].

4. Conclusions

The ELP represents a valuable technique to produce the controlled deposition of Pd on carbon fibers; instead, on the ceramic support, the formation of films was observed on some fibers, thus decreasing the performance of these catalysts for nitrite conversion. The best solid for the nitrite reduction was Pd on carbon fiber with 1.8 wt.% of Pd (B1). Its good performance could be associated with the homogeneous deposition of a great quantity of Pd particles with small size (130–210 nm). The lower activity of the ceramic support for this reaction could be due to the low availability of Pd

surface sites on the films. Besides, both supports were very selective to nitrogen formation.

Acknowledgments

The authors wish to acknowledge the financial support received from ANPCyT (BID PICT no. 2008-1053), UNL and CONICET from Argentina. Thanks are given to Elsa Grimaldi for the English language editing.

References

- [1] M.L. Bosko, F.A. Marchesini, L.M. Cornaglia, E.E. Miró, *Catalysis Communications* 16 (2011) 189–193.
- [2] K.D. Beard, J.W. Van Zee, J.R. Monnier, *Applied Catalysis B* 88 (2009) 185–193.
- [3] J.K. Chinthaginjala, L. Lefferts, *Applied Catalysis B* 101 (2010) 144–149.
- [4] S.D. Ebbesen, B.L. Mojet, L. Lefferts, *Journal of Catalysis* 256 (2008) 15–23.
- [5] D. Gasparovicová, M. Králik, M. Hronec, Z. Vallusová, H. Vinek, B. Corain, *Journal of Molecular Catalysis A* 264 (2007) 93–102.
- [6] F.A. Marchesini, N. Picard, E.E. Miró, *Catalysis Communications* 21 (2012) 9–13.
- [7] S.R. de Miguel, J.I. Vilella, E.L. Jablonski, O.A. Scelza, C. Salinas-Martínez de Lecea, A. Linares-Solano, *Applied Catalysis A* 232 (2002) 237–246.
- [8] P.P. Mardilovich, Y. She, Y.H. Ma, M. Rei, Defect-free palladium membranes on porous stainless-steel support, *AIChE Journal* 44 (1998) 310–322.
- [9] F.A. Marchesini, L.B. Gutierrez, C.A. Querini, E.E. Miró, *Chemical Engineering Journal* 159 (2010) 203–211.
- [10] U. Matatov-Meytal, M. Sheintuch, *Catalysis Communications* 10 (2009) 1137–1141.
- [11] Y.S. Cheng, K.L. Yeung, *Journal of Membrane Science* 158 (1999) 127–141.
- [12] M.L. Bosko, J.B. Miller, E.A. Lombardo, A.J. Gellman, L.M. Cornaglia, *Journal of Membrane Science* 369 (2011) 267–276.
- [13] M. Brun, A. Berthet, J.C. Bertolini, *Journal of Electron Spectroscopy and Related Phenomena* 104 (1999) 55–60.
- [14] A.E. Palomares, C. Franch, A. Corma, *Catalysis Today* 149 (2010) 348–351.
- [15] M.E. Ayturk, Y.H. Ma, *Journal of Membrane Science* 330 (2009) 233–245.
- [16] H. Ma, Z. Liu, L. Wu, Y. Wang, X. Wang, *Thin Solid Films* 519 (2011) 7860–7863.
- [17] L. Lemaignan, C. Tong, V. Begon, R. Burch, D. Chadwick, *Catalysis Today* 75 (2002) 43–48.
- [18] F.A. Marchesini, S. Irusta, C.A. Querini, E.E. Miró, *Catalysis Communications* 9 (2008) 1021–1026.
- [19] Y.A. Ryndin, M.V. Stenin, A.I. Boronin, V.I. Bukhtiyarov, V.I. Zaikowskii, *Applied Catalysis A* 54 (1989) 277–288.
- [20] F. Coloma, J. Narciso-Romero, A. Sepúlveda-Escribano, F. Rodríguez-Reinoso, *Carbon* 36 (7–8) (1998) 1011–1019.
- [21] O.S.G.P. Soares, J.J.M. Órfão, J. Ruiz-Martínez, J. Silvestre-Albero, A. Sepúlveda-Escribano, M.F.R. Pereira, *Chemical Engineering Journal* 165 (2010) 78–88.
- [22] O.S.G.P. Soares, J.J.M. Órfão, M.F.R. Pereira, *Applied Catalysis B* 102 (2011) 424–432.
- [23] Council Directive 98/83/EC of 3 November 1998 on the quality of water intended for human consumption. <http://www.iss.it/binary/publ/publi/0016.1109850012.pdf>. Rapport ISTISAN 00/16, 2000.
- [24] O.S.G.P. Soares, J.J.M. Órfão, M.F.R. Pereira, *Catalysis Letters* 126 (2008) 253–260.
- [25] F.A. Marchesini, S. Irusta, C. Querini, E. Miró, *Applied Catalysis A* 348 (2008) 60–70.